中國機械工程學刊第三十九卷第五期第 443~450 頁(民國一百零七年)
Journal of the Chinese Society of Mechanical Engineers, Vol.39, No.5, pp 443~450 (2018)

Chaos Control in Attitude Dynamics of Automotive Disc Brake System Based on Synchronization

Shun-Chang Chang*

Keywords：disc brake, bifurcation, chaos, Lyapunov exponent, synchronization.

ABSTRACT

Disc brake squeal is a nonlinear transient phenomenon of the friction-induced self-excited instability of an automotive brake system. In most situations, decreasing this squeal noise to some extent during braking is very important for the comfort of passengers, which is dependent on an absence of chaos; consequently, suppressing chaos becomes quite important. Therefore, this study aims to confirm chaotic motion and apply synchronization to control chaos for an automotive disc brake system. Rich dynamics of the disc brake system were studied using a bifurcation diagram, phase portraits, a Poincaré map, frequency spectra, and Lyapunov exponents. First, the largest Lyapunov exponent was estimated using synchronization to identify periodic and chaotic motions. Next, complex nonlinear behaviors were thoroughly observed for a range of parameter values in the bifurcation diagram. Finally, a continuous feedback control method based on synchronization characteristics was proposed to eliminate chaotic oscillations, improve the performance of the automotive disc brake system, and prevent brake squeal noise from occurring. Numerical simulations were utilized to verify the feasibility and efficiency of the proposed control technique.

INTRODUCTION

In many engineering applications, dry friction, clearance, and impact factors often result in a sudden change of the vector fields describing the dynamic behaviors of mechanical systems. These systems are not smooth, and are referred to as non-smooth dynamical systems. Dry friction is a typical non-smooth factor and plays an important role in engineering applications. It is a source of self-sustained oscillations, which are referred to as stick-slip oscillations. These oscillations often cause some undesired effects observed in engineering applications, including the noise of a squeaking automotive windshield wiper (Chang and Lin, 2004) and the action of squealing brakes.

In the automotive industry, brake squeal has become an important cost factor due to customer dissatisfaction and it has been a challenging issue for many engineers and researchers due to its immense complexity. A great deal of research has focused on brake squeal using a variety of analysis and experimental methods (Quyang et al., 1992; Ahmed, 2012; Chen, 2007; Kinkaid et al., 2003; Kang, 2012; Oberst et al., 2013). The analysis of automotive disc brake squeal performed by Ouyang et al., leads to an important conclusion: chattering behavior is a self-excited vibration based on a stick-slip phenomenon and exists only in a certain range of friction parameters. Beyond this range, chatter vibrations no longer occur. This property is a feature of the stick-slip phenomenon that can be observed in other physical systems (Tarng and Cheng, 1995; Mokhtar et al., 1998; Oancea and Laursen, 1998; Awrejcewicz et al., 2005). Much progress and insight have been gained in recent years and brakes have become quieter. However, squealing still occurs frequently, and therefore, much still needs to be understood and done. The dynamic behaviors of the disc brake system can be investigated to find an effective way of controlling brake vibrations and squealing noises. Thus, noise generation and suppression have become important factors in the design and manufacture of brake components.

It is well known that brake squeal is a nonlinear transient phenomenon and a number of studies using analytical and experimental models of brake systems indicate that it can be treated as chaotic motion (Oberst and Lai, 2011; Shin et al., 2002a, b). Shin et al. (2002a, b) showed that a forced two-degree-of-freedom (2 - DOF), dry friction

Paper Received December, 2016. Revised Sepfember, 2017. Accepted August, 2018, Author for Correspondence: Shun-Chang Chang.

* *Professor, Department of Mechanical and Automation Engineering, Da-Yeh University, No. 168, University Road, Dacun, Changhua 51591, TAIWAN (R.O.C.)*

analysis model with negative-velocity gradient characteristics developed chaotic pad motion when frequencies of the pad and the disc were close to each other. Various numerical features such as bifurcation diagrams, phase portraits, Poincaré maps, frequency spectra, and Lyapunov exponents can be presented to observe periodic and chaotic motions. For a broad range of parameters, the Lyapunov exponent provides the most powerful means of measuring the sensitivity of a dynamical system to its initial conditions. It can be used to determine whether a system is in chaotic motion. The algorithms for computing Lyapunov exponents of smooth dynamical systems are well established (Shimada and Nagashima, 1979; Wolf et al., 1985; Benettin et al., 1980a, b). However, some non-smooth dynamical systems have discontinuities where this algorithm cannot be directly applied, such as those associated with dry friction, backlash, or impact. Many works have proposed methods for calculating the Lyapunov exponents of non-smooth dynamical systems (Muller, 1995; Hinrichs et al., 1997; Stefanski, 2000). The method proposed by Stefanski (2000) for estimating the largest Lyapunov exponent for a disc brake system is employed in this study.

Although some chaotic behavior may be acceptable, it is generally undesirable as it degrades performance and restricts the operating range of many electrical and mechanical devices. Recently, the control of a chaotic stick-slip mechanical system has advanced considerably and various techniques have been proposed (Galvanetto, 2001; Dupont, 1991; Feeny and Moon, 2000). Galvanetto (2001) applied adaptive control to unstable periodic orbits embedded in chaotic attractors of some discontinuous mechanical systems. Feeny and Moon (2000) used high-frequency excitation, or dither, to quench stick-slip chaos. A chaotic motion must be controlled to a periodic orbit in a steady state to improve the disc brake system's performance and eliminate chatter vibration in an automotive disc brake. For this purpose, a continuous feedback control method proposed by Pyragas (1992) and Kapitaniak (1995) is used in this paper to convert chaos into periodic motion through the adaptation of combined feedback with a periodic external force in a special form in chaotic systems. Some numerical simulation results are presented to establish the feasibility of the proposed method.

MODEL DESCRIPTION

The basic dynamics of brake squeal noise can be understood using a 2-DOF model as shown in Fig. 1 (Shin et al., 2002a, b). The system with subscript 1 denotes the pad, the system with subscript 2 denotes the disc, and m, k, and c denote mass, stiffness, and damping, respectively. The motion of the first mass (m_1) represents the tangential motion of the pad and the motion of the second mass (m_2) represents the in-plane motion of the disc. The normal force acting on the interface is $N = P \times S$ where P is the pressure applied and S is the surface area of the interface. The resulting frictional force F_f is dependent on the normal force and the dynamic coefficient of friction between the two sliding surfaces. The disc motion is the superposition of a constant imposed velocity v_0 and velocity $\dot{x}_d$, and the pad motion has velocity $\dot{x}_p$.

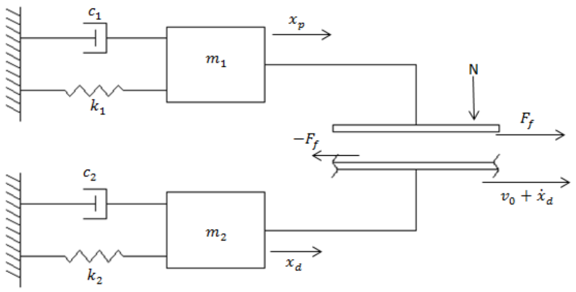

Fig. 1. Schematic diagram of an automotive disc brake system.

The motion of the system is governed by a static frictional force during stick motion and by a velocity-dependent frictional force during slip motion. For the stick mode, the stick friction force is limited by the maximum state friction force, i.e., $|F_s| \le \mu_s N$, and is balanced with the reaction forces acting on the masses. To conduct this study a linear friction model for the interface is used, and this is shown as a function of the relative velocity v_r between the pad and the disc. μ_s is the static friction coefficient and $\mu(v_r)$ is the dynamic friction coefficient, i.e., $\mu(v_r) = \mu_s - \alpha|v_r|$. The negative gradient of the dynamic frictional coefficient is α. By considering the relative motion between the two masses, the static frictional force can be written as:

$$F_s = k_1 x_p + c_1 \dot{x}_p - k_2 x_d - c_2 \dot{x}_d, \quad (1)$$

and the frictional force can be described by:

$$F_f = \begin{cases} \min(|F_s|, \mu_s N) \cdot \mathrm{sgn}(F_s), & \text{for } v_r = 0 \text{ stick}, \\ \mu(v_r) N \cdot \mathrm{sgn}(v_r), & \text{for } v_r \ne 0 \text{ slip}. \end{cases} \quad (2)$$

For numerical analysis, the frictional force is switched appropriately according to the type of motion. Also, a region of small band for the relative velocity is defined, i.e., $|v_r| < \varepsilon$, where $\varepsilon \ll v_0$. Thus, the equations of motion become:

$$m_1 \ddot{x}_p + c_1 \dot{x}_p + k_1 x_p = F_f(v_r) - F_f(v_0), \quad (3a)$$
$$m_1 \ddot{x}_d + c_2 \dot{x}_d + k_2 x_d = -[F_f(v_r) - F_f(v_0)], \quad (3b)$$

where $v_r = v_0 + \dot{x}_d - \dot{x}_p$, and a constant, $F_f(v_0) = N(\mu_s - \alpha v_0)$, is introduced to compensate for any offset. Considering the friction model, Eq. (3) can be written in the form of state equations to facilitate computation as follows:

$$\dot{x}_1 = x_2, \quad \text{(4a)}$$
$$\dot{x}_2 = -\frac{c_1}{m_1}x_2 - \frac{k_1}{m_1}x_1 + \frac{1}{m_1}(F_f(v_r) - F_f(v_0)), \quad \text{4(b)}$$
$$\dot{x}_3 = x_4, \quad \text{4(c)}$$
$$\dot{x}_4 = -\frac{c_2}{m_2}x_4 - \frac{k_2}{m_2}x_3 - \frac{1}{m_2}(F_f(v_r) - F_f(v_0)), \quad \text{4(d)}$$

where $x_p = x_1$, $\dot{x}_p = \dot{x}_1 = x_2$, $x_d = x_3$, $\dot{x}_d = \dot{x}_3 = x_4$. Table 1 presents the values of the parameters used in the above equations.

Table 1. Physical parameters of a disc brake system.

Nomenclature	Value
m_1: mass of the pad	1.0
m_2: mass of the disc	1.0
k_1: stiffness of the pad	1.0
k_2: stiffness of the disc$_\theta$	3.0
c_1: damping coefficient of the pad	
c_2: damping coefficient of the disc	
v_r: relative velocity between the pad and the disc	
x_p, x_d: displacement variables of pad and disc respectively	
$\dot{x}_p, \dot{x}_d$: velocity variables of pad and disc respectively	
μ_s: static friction coefficient	0.6
v_0: constant driving speed of the disc	1.0
N: normal force	10.0
α: the negative gradient of the dynamic friction coefficient	0.03
ε: a region of small band for the relative velocity that defines the stick motion	10^{-5}
$\mu(v_r)$: dynamic friction coefficient dependent on the relative velocity	
K: feedback gain	

THE OVERALL CHARACTERISTICS OF THE SYSTEM AND CHAOTIC ATTITUDE MOTION

A series of numerical simulations based on Eq. (4) was performed to clearly understand the characteristics of the proposed system. Figure 2 shows the resulting bifurcation diagram, which comprehensively explains the dynamic behavior over a range of parameter values. A bifurcation diagram is widely used to describe transitions from periodic to chaotic motion in dynamical systems. The commercial package DIVPRK of IMSL in FORTRAN subroutines for mathematics applications was used to solve these ordinary differential equations (IMSL, Inc., 1989). This figure clearly indicates that the chaotic motions appear approximately in region III. Period-$2n$ orbits appear in region II and period-1 orbits occur in region I. The Poincaré map is constructed by viewing the phase space diagram stroboscopically in a way such that motion is observed periodically. The phase portrait evolves from a set of trajectories emanating from various initial conditions in the state space. When the solution reaches a stable state, the asymptotic behavior of the phase trajectories is particularly interesting and the transient behavior in the system is ignored. A frequency spectrum can also be employed to identify and characterize the system. It is often used to distinguish between periodic, quasi-periodic, and chaotic motion in dynamical systems. A stable periodic motion is present in region I. Each response is characterized by a phase portrait, a Poincaré map (velocity vs. phase angle), and a frequency spectrum. Figure 3 indicates that the equilibrium point of Eq. (4) is stable if the parameter (damping coefficient) lies in region I. When the parameter (damping coefficient) lies in region II, period-doubling bifurcations appear. Figure 4 shows that a cascade of period-doubling bifurcations causes a series of subharmonic components, which show the bifurcations with the new frequency components at Ω/2, 3Ω/2, 5Ω/2, … ect. As the parameter (damping coefficient) continues to decrease into region III in Fig. 2, a cascade of period-doubling bifurcations, which lead to chaotic motion, are clearly visible. Therefore, chatter vibration occurs. Two descriptors, namely the Poincaré map and the frequency spectrum, characterize the essence of the chaotic behavior. The Poincare map shows an infinite set of points that are collectively referred to as a strange attractor. The frequency spectrum of chaotic motion contains a broad band. These two features of the strange attractor and the continuous type Fourier spectrum are strong indicators of chaos. Figure 5 clearly shows chaotic behaviors in regions III. Figures (5a–5c) present the phase portraits, Poincaré maps, and frequency spectra, respectively.

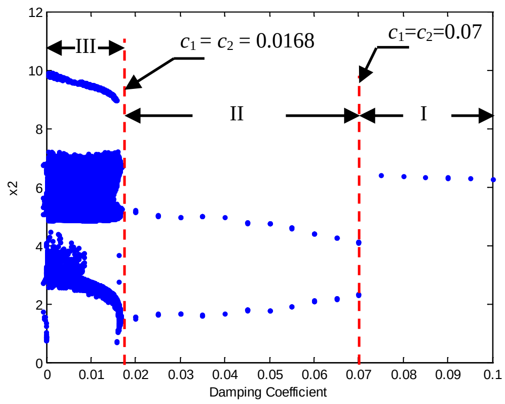

Fig. 2. Bifurcation diagram of the velocity of the disc versus the damping coefficient.

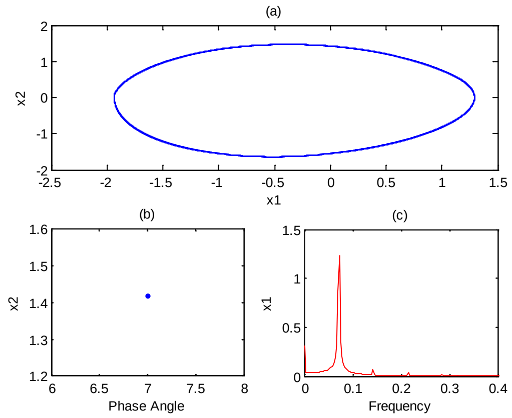

Fig. 3. Period-1 orbit for $c_1 = c_2 = 0.075$: (a) Phase portrait; (b) Poincare map; (c) Frequency spectrum.

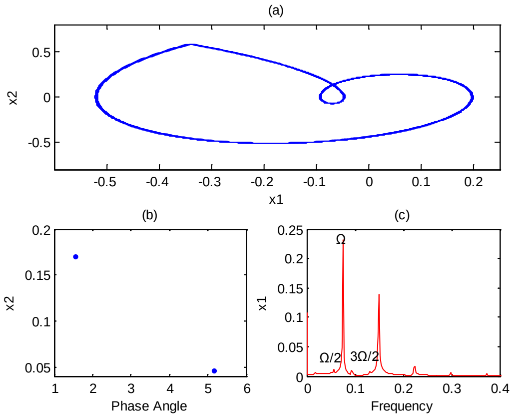

Fig. 4. Period-2 orbit for $c_1 = c_2 = 0.02$: (a) Phase portrait; (b) Poincare map; (c) Frequency spectrum.

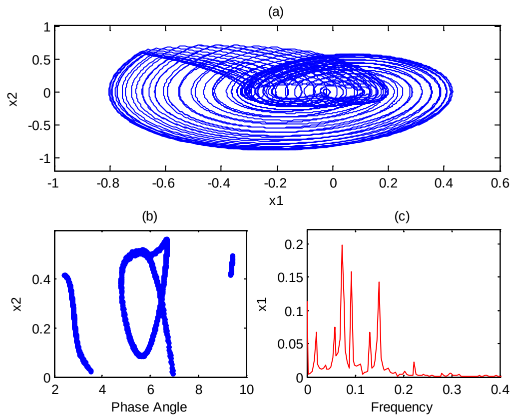

Fig. 5. Chaotic motion for $c_1 = c_2 = 0.01$: (a) Phase portrait; (b) Poincare map; (c) Frequency spectrum.

ESTIMATION OF THE LARGEST LYAPUNOV EXPONENT

The largest Lyapunov exponent is one of the most useful indicators for chaotic system diagnostics. Every dynamical system has a spectrum of Lyapunov exponents (λ) that determine how the length, area, and volumes change in the phase space. In other words, Lyapunov exponents measure the rate of divergence (or convergence) of two initially nearby orbits. Chaos can be identified by simply calculating the largest Lyapunov exponent, thus determining whether nearby trajectories diverge ($\lambda > 0$) or converge ($\lambda < 0$) on average. Any bounded motion in a system containing at least one positive Lyapunov exponent is defined as chaotic, while non-positive Lyapunov exponents indicate periodic motion.

Algorithms for computing the Lyapunov spectrum of "smooth" dynamical systems are well established (Shimada and Nagashima, 1979; Wolf et al., 1985; Benettin et al., 1980a, b). However, "non-smooth" dynamical systems with discontinuities such as dry friction, backlash or stick-slip prevent this algorithm from being applied directly. The disc brake is simply a system that is subjected to a dry-friction force. Hence, this study demonstrates the chaotic behavior of an automotive disc brake system by computing the largest Lyapunov exponent. Stefanski (2000) recently recommended a simple method for estimating the largest Lyapunov exponent based on synchronization properties. The synchronization of two distinct systems, which may have identical structures or may be completely different, has recently aroused particular interest. The synchronization controls the response system using the output of the drive system, so that the output of the response system asymptotically follows the output of the drive system.

Stefanski's (2000) method for estimating the largest Lyapunov exponent is described briefly herein as follows.

The dynamical system is decomposed into the following two subsystems:

drive system

$$\dot{p} = f(p), \tag{8}$$

response system

$$\dot{q} = f(q). \tag{9}$$

Consider a dynamical system that comprise two identical n-dimensional subsystems; a coupling coefficient d is applied only to the response system (8), while the drive system remains unchanged. The first order differential equations describing such a system can be expressed as,

$$\begin{aligned} \dot{p} &= f(p), \\ \dot{q} &= f(q) + d(p-q). \end{aligned} \tag{10}$$

The condition of synchronization (Eq. (10)) is given by the inequality

$$d > \lambda_{\max} . \quad (11)$$

The smallest value of the coupling coefficient d in synchronization d_S is assumed to be equal to the maximum Lyapunov exponent as follows:

$$d_s = \lambda_{\max} . \quad (12)$$

Eq. (10) obtains the augmented system based on Eq. (4) as follows:

$$\begin{aligned}
\dot{p}_1 &= p_2,\\
\dot{p}_2 &= -\tfrac{c_1}{m_1}p_2 - \tfrac{k_1}{m_1}p_1 + \tfrac{1}{m_1}(F_f(v_r) - F_f(v_0)),\\
\dot{p}_3 &= p_4,\\
\dot{p}_4 &= -\tfrac{c_2}{m_2}p_4 - \tfrac{k_2}{m_2}p_3 - \tfrac{1}{m_2}(F_f(v_r) - F_f(v_0)).\\
\dot{q}_1 &= q_2 + d(p_1 - q_1),\\
\dot{q}_2 &= -\tfrac{c_1}{m_1}q_2 - \tfrac{k_1}{m_1}q_1 + \tfrac{1}{m_1}\left(\tilde{F}_f(\tilde{v}_r) - F_f(v_0)\right) + d(p_2 - q_2),\\
\dot{q}_3 &= q_4 + d(p_3 - q_3),\\
\dot{q}_4 &= -\tfrac{c_2}{m_2}q_4 - \tfrac{k_2}{m_2}q_3 - \tfrac{1}{m_2}\left(\tilde{F}_f(\tilde{v}_r) - F_f(v_0)\right) + d(p_4 - q_4),
\end{aligned} \quad (13)$$

where

$$\tilde{v}_r = v_0 + q_4 - q_2$$
$$\tilde{\mu}(\tilde{v}_r) = \mu_s - \alpha\tilde{v}_r$$
$$\tilde{F}_s = k_1q_1 + c_1q_2 - k_2q_3 - c_2q_4,$$
$$\tilde{F}_f = \begin{cases} \min\left(|\tilde{F}_s|, \mu_s N\right)\cdot \operatorname{sgn}(\tilde{F}_s), & \text{for } \tilde{v}_r = 0 \text{ stick},\\ \tilde{\mu}(\tilde{v}_r)N\cdot \operatorname{sgn}(\tilde{v}_r), & \text{for } \tilde{v}_r \neq 0 \text{ slip}. \end{cases} \quad (14)$$

The maximum Lyapunov exponent of the system is then determined for the chosen parameter values as described above. Figure 6 presents the results of the numerical calculations showing the largest Lyapunov exponents obtained using the described synchronization method. The system exhibits chaotic motion since all the largest Lyapunov exponents are positive for damping coefficients $c_1 = c_2 < 0.0168$.

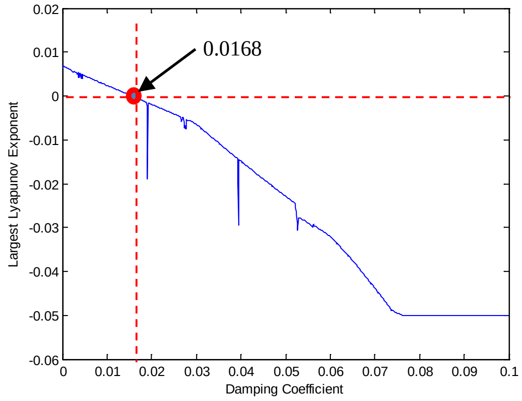

Fig. 6. Evolution of the largest Lyapunov exponent.

CONTROLLING CHAOS BY SYNCHRONIZATION

Learning to predict the behaviors of a chaotic system can be beneficial; however, the ultimate objective is to assume control of the system. Avoiding chaotic phenomena to enhance the performance of dynamic systems requires that chaotic motion be transformed into periodic motion. Suitable control methods must therefore be developed. Pyragas (1992) and Kapitaniak (1995) proposed a simple and effective time-continuous control method that converts chaos into periodic motion by constructing a special form of a time-continuous perturbation and a feedback mechanism. Figure 7 shows the proposed feedback controlling loop with the external periodic perturbation. This method is explained briefly below.

Consider an n-dimensional dynamical system:

$$\dot{z} = P(z) , \quad (15)$$
$$\dot{y} = Q(y) + F(t) , \quad (16)$$

where $z(t), y(t) \in R^n$ is the state vector, and $F(t)$ denotes the input signal. Without an input signal ($F(t) = 0$), the considered system (16) is assumed to have a stranger attractor, while system (15) is a periodic system. Usually, the periodic system is referred to as the drive system and the chaotic system as the response system. These two distinct systems were synchronized using the strategy shown in Fig. 7. The difference between the signals $y(t)$ and the signals $z(t)$ are used as a control signal,

$$F(t) = K[y(t) - z(t)] , \quad (17)$$

which is introduced into the chaotic system (16) as a negative feedback. In Eq. (17), K represents feedback gain.

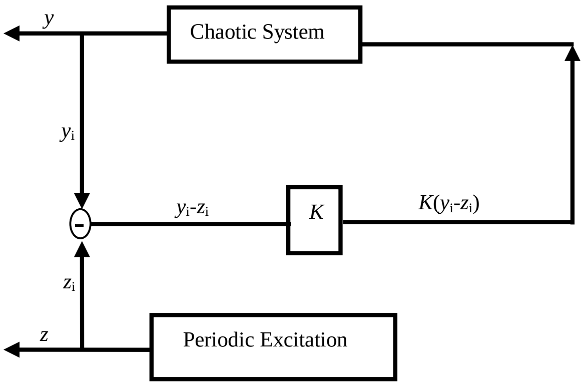

Fig. 7. Block diagram of the continuous chaos control method.

When $c_1 = c_2 = c_z = 0.1$ is selected for the drive system, Eq. (4) reveals period-1 motion.

$$\dot{z}_1 = z_2, \tag{18a}$$
$$\dot{z}_2 = -\frac{c_z}{m_1}z_2 - \frac{k_1}{m_1}z_1 + \frac{1}{m_1}(F_f(v_r) - F_f(v_0)), \tag{18b}$$
$$\dot{z}_3 = z_4, \tag{18c}$$
$$\dot{z}_4 = -\frac{c_z}{m_2}z_4 - \frac{k_2}{m_2}z_3 - \frac{1}{m_2}(F_f(v_r) - F_f(v_0)). \tag{18d}$$

When $c_1 = c_2 = c_y = 0.01$ is selected for the response system, Eq. (4) reveals chaotic motion.

$$\dot{y}_1 = y_2, \tag{19a}$$
$$\dot{y}_2 = -\frac{c_y}{m_1}y_2 - \frac{k_1}{m_1}y_1 + \frac{1}{m_1}(F_f(v_r) - F_f(v_0)), \tag{19b}$$
$$\dot{y}_3 = y_4, \tag{19c}$$
$$\dot{y}_4 = -\frac{c_y}{m_2}y_4 - \frac{k_2}{m_2}y_3 - \frac{1}{m_2}(F_f(v_r) - F_f(v_0)). \tag{19d}$$

A control signal Eq. (17) was introduced into Eq. (19) as feedback control to synchronize Eqs. (18) and (19).

When incorporated into Eq. (19), the control signal Eq. (17) yielded the following coupled system, which is capable of achieving synchronization:

$$\dot{y}_1 = y_2 + K(y_1 - z_1), \tag{20a}$$
$$\dot{y}_2 = -\frac{c_y}{m_1}y_2 - \frac{k_1}{m_1}y_1 + \frac{1}{m_1}\left(F_f(v_r) - F_f(v_0)\right) + K(y_2 - z_2), \tag{20b}$$
$$\dot{y}_3 = y_4 + K(y_3 - z_3), \tag{20c}$$
$$\dot{y}_4 = -\frac{c_y}{m_2}y_4 - \frac{k_2}{m_2}y_3 - \frac{1}{m_2}\left(F_f(v_r) - F_f(v_0)\right) + K(y_4 - z_4). \tag{20d}$$

Eq. (20) reveals chaotic motion when $K = 0$ and $c_y = 0.01$. Adjusting the feedback gain $K > 0.024$ converts the dynamics of system (20) from chaotic motion into periodic motion. Figure 8 presents the resulting bifurcation diagram, which comprehensively explains the dynamic behavior over a range of feedback gains. Chaotic motion appeared when $K \le 0.024$ and periodic motion appeared when $K > 0.024$. Accordingly, if the chaotic motions were converted into periodic motions, then the feedback gain should be selected to satisfy the condition $K > 0.024$. The chaotic disc brake system (19) can be synchronized by applying the control signal. Thus, this chaotic disc brake system can be managed using the control signal ($K = 0.05$), such that chaotic motion is converted into period-2 motion. The control signal is introduced after $t = 200$ s. Figure 9 presents the time response and phase portrait for $K = 0.05$.

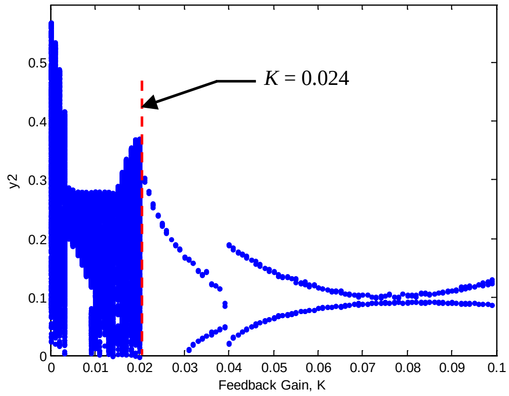

Fig. 8. Bifurcation diagram of a system with continuous control, where K is the feedback gain.

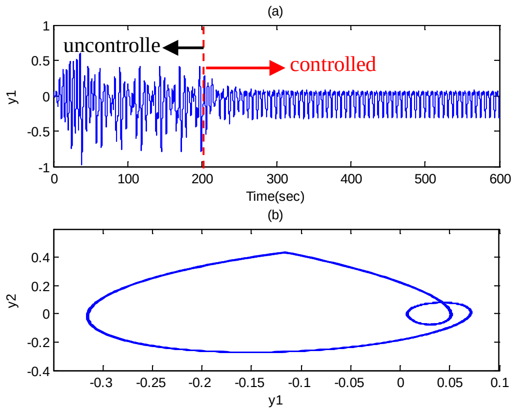

Fig. 9. Controlling chaotic motion ($c_1 = c_2 = 0.01$) to a desired period-two orbit for $K = 0.05$: (a) time response of the displacement; (b) phase portrait of the controlled system (20), the control signal is added after 200 s.

CONCLUSIONS

This investigation studied complex nonlinear behavior and the chaos control problem on an automotive disc brake system. Numerical methods including time responses, Poincaré maps, frequency spectra, and the largest Lyapunov exponent were employed to obtain the characteristics of the nonlinear disc brake system. The resulting bifurcation diagram showed many nonlinear dynamics and chaotic phenomena, revealing that the disc brake system exhibits chaotic motion at lower damping coefficients. Nonlinear analysis using a 2-DOF model has been presented to demonstrate the rich nonlinear dynamics of the disc brake squeal noise and to show the importance of damping. The Lyapunov exponent is a very powerful tool for determining whether a system exhibits chaotic motion. The largest Lyapunov exponent of the disc brake system was estimated from the properties of its synchronization phenomenon. Finally, a continuous control method based on synchronization characteristics was applied to suppress chaotic motion, improve the performance of the disc brake system, and prevent brake squeal noise from occurring.

ACKNOWLEDGMENT

This research was supported by the National Science Council in Taiwan, Republic of China, under project number NSC 102-2632-E-212 -001 -MY3.

REFERENCES

Ahmed, I., "Analysis of Ventilated Disc Brake Squeal Using a 10 DOF Model," *SAE Paper*, 2012-01-1827 (2012).

Awrejcewicz, J., Dzyubak, L. and Grebogi, C., "Estimation of Chaotic and Regular (Stick-slip and Slip-slip) Oscillations Exhibited by Coupled Oscillators with Dry Friction," *Nonlinear Dynamics*, Vol. 42, pp. 383-394 (2005).

Benettin, G., Galgani, L., Giorgilli, A. and Strelcyn, J.M., "Lyapunov Exponents for Smooth Dynamical Systems and Hamiltonian Systems; a Method for Computing all of them," Part I: theory. *Meccanica*, Vol. 15, pp. 9-20 (1980a).

Benettin, G., Galgani, L., Giorgilli, A. and Strelcyn, J.M., "Lyapunov Exponents for Smooth Dynamical Systems and Hamiltonian Systems; a Method for Computing all of them," Part II: Numerical Application. *Meccanica*, Vol. 15, pp. 21-30 (1980b).

Chang, S.C. and Lin, H.P., "Chaos Attitude Motion and Chaos Control in an Automotive Wiper System," *Int. J. Solids Struct.*, Vol. 41, pp. 3491-3504 (2005).

Chen, F., "Disc Brake Squeal: an Overview," *SAE Paper*, 2007-01-0587 (2007).

Dupont, P.E., "Avoiding stick-slip in position and force control through feedback, " Proc. of the IEEE International Conference on Robotics and Automation, Sacramento, CA, USA (1991)

Feeny, B.F. and Moon, F.C., "Quenching Stick-slip Chaos with Dither," *J. Sound Vib.*, Vol. 273, pp. 173-180 (2000).

Galvanetto, U., "Flexible Control of Chaotic Stick-slip Mechanical Systems," *Comp. Meth. Appl. Mech. Engine.*, Vol. 190, pp. 6075-6087 (2001).

Hinrichs, N., Oestreich, M. and Popp, K., "Dynamics of Oscillators with Impact and Friction," *Chaos Solitons Fract.*, Vol. 8, pp. 535-558 (1997).

IMSL Inc. User manual-IMSL/LIBRARY, vol.2. (1989).

Kang, J., "Finite Element Modelling for the Investigation of in-plane Modes and Damping Shims in Disc Brake Squeal," *J. Sound Vib.*, Vol. 331, pp. 2190-2202 (2012).

Kapitaniak, T., "Continuous Control and Synchronization in Chaotic Systems," *Chaos Solitons Fract.*, Vol. 6, pp. 237-244 (1995).

Kinkaid, N.M., O'Reilly, O.M. and Papadopoulos, P., "Automotive Disc Brake Squeal," *J. Sound Vib.*, Vol. 267, pp. 105-166 (2003).

Mokhtar, M.O.A., Younes, Y.K. and Mahdy, T.H.EI. and Attia, N.A., "A Theoretical and Experimental Study on the Dynamics of Sliding Bodies with Dry Conformal Contacts," *Wear*, Vol. 218, pp. 172-178 (1998).

Muller, P., "Calculation of Lyapunov Exponents for Dynamical Systems with Discontinuities," *Chaos Solitons Fract.*, Vol. 5, pp. 1671-1681 (1995).

Oancea, V.G. and Laursen, T.A., "Investigations of Low Frequency Stick-slip Motion: Experiments and Numerical Modelling," *J. Sound Vib.*, Vol. 213, pp.577-600 (1998).

Oberst, S. and Lai, J.C.S., "Chaos in Brake Squeal Noise," *J. Sound Vib.*, Vol. 330, pp. 955-975 (2011).

Oberst, S., Lai, J.C.S. and Marburg, S., "Guidelines for Numerical Vibration and Acoustic Analysis of Disc Brake Squeal Using Simple Models of Brake Systems," *J. Sound Vib.*, Vol. 332, pp. 2284-2299 (2013).

Ouyang, H., Nack, W., Yuan, Y. and Chen, F., "Numerical Analysis of Automotive Disc Brake Squeal: a Review," *Int. J. Vehicle Noise Vib.*, Vol. 1, pp. 207-231 (1992).

Pyragas, K., "Continuous Control of Chaos by Self-controlling Feedback," *Phys. Lett. A*, Vol. 170, pp. 421-428 (1992).

Shimada, I. and Nagashima, T., "A Numerical Approach to Ergodic Problems of Dissipative Dynamical Systems," *Prog. Theor. Phys.*, Vol. 61, pp. 1605-1616 (1979).

Shin, K., Brennan, M.J. and Harris, C.J., "Analysis of Disc Brake Noise Using a Two-degree-of-freedom Model," *J. Sound Vib.*, Vol. 254, pp. 837-848 (2002a).

Shin, K., Oh, J.E. and Brennan, M.J., "Nonlinear Analysis of Friction Induced Vibrations of a Two-degree-of-freedom Model for Disc Brake Squeal," *JSME Int. J. C-Mech. Sy.*, Vol. 45, pp.

426-432 (2002b).
Stefanski, A., "Estimation of the Largest Lyapunov Exponent in Systems with Impact," *Chaos Solitons Fract.*, Vol. 11, pp. 2443-2451 (2000).
Tarng, Y.S. and Cheng, H.E., "An Investigation of Stick-slip Friction on the Contouring Accuracy of CNC Machine Tools," *Int. J. Mach. Tool Manu.*, Vol. 35, pp. 565-576 (1995).
Wolf, A., Swift, J.B., Swinney, H.L. and Vastano, J.A., "Determining Lyapunov Exponents from a Time Series," *Physica D*, Vol. 16, pp. 285-317 (1985).

基於同步化應用於車輛碟式煞車系統之渾沌控制

張舜長
大葉大學機械與自動化工程學系

摘 要

車輛碟式煞車所產生的尖銳聲音是由摩擦力導致的一種非線性現象。，降低在煞車時的尖銳聲對乘客舒適性而言是很重要的，而此現象造成因素是煞車系統產生渾沌運動所致。因此，本文旨在探討碟式煞車系統的非線性動態。藉由分歧圖、相圖、龐克映相圖、頻譜圖及李亞譜諾指數來呈現其非線性行為。利用最大的李亞譜諾指數來驗證系統是否有存在渾沌行為。最後，採用同步化法及連續控制法去控制渾沌運動，並經由數值模擬結果顯示，所提出的控制方式皆能有效地控制煞車系統渾沌行為的發生並能將之轉換為穩定的周期運動，以抑制煞車時產生的尖銳聲。。